Aalborg Universitet

AALBORG UNIVERSITY

From Consumption to Prosumption - Operational Cost Optimization for Refrigeration System With Heat Waste Recovery

Minko, Tomasz; Garcia, Jesus Lago; Bendtsen, Jan Dimon; Wisniewski, Rafal; Izadi-Zamanabadi, Roozbeh

From Consumption to Prosumption - Operational Cost Optimization for Refrigeration System With Heat Waste Recovery

Tomasz Minko * **Jesus Lago Garcia** ** **Jan Dimon Bendtsen** *
Rafael Wisniewski * **Roozbeh Izadi-Zamanabadi** ***

* *Automation and Control, Aalborg University, Denmark (e-mail: tmi@es.aau.dk, dimon@es.aau.dk, raf@es.aau.dk).*
** *Delft Center for Systems and Control, Delft University of Technology, Netherlands (e-mail: j.lagogarcia@tudelft.nl).*
*** *Danfoss A/S, Denmark (e-mail: roozbeh@danfos.com).*

Abstract: Implementation of a liquid cooling transforms a refrigeration system into a combined cooling and heating system. Reclaimed heat can be used for building heating purposes or can be sold. Carbon dioxide based refrigeration systems are considered to have a particularly high potential for becoming efficient heat energy producers. In this paper, a CO_2 system that operates in the subcritical region is examined. The modelling approach is presented, and used for operation optimisation by way of non-linear model predictive control techniques. Assuming that the heat is sold, it turns out that the system has negative operational cost. Depending on the choice of objective function daily revenue varies from about 7.9 [*eur*] to 11.9 [*eur*].

1. INTRODUCTION

Prosumption is a term that describes the ability of an entity to not only consume but also produce power. Note that power is a general notion; here, we specifically consider electrical and thermal power. In this paper, we take a one evaporator, one gas cooler CO_2 supermarket refrigeration system as an example of an electrical power consumer. Cooling of the hot side refrigerant is typically done by air fans, but this solution is very inefficient since all the heat is exhausted into the ambient and simply wasted. Implementation of a liquid cooling system would instead transform such a refrigeration system into a combined heat and cooling (CHC) system, where the excess heat of the hot side refrigerant could be reclaimed, stored and either used for in-house purposes, or sold to nearby households.

1.1 State Of The Art

In this paper optimal control of such a system is examined. Given some appropriate cost $L(x, u)$ in (1a), the optimal control problem (OCP), defined for a given initial point $\bar{x}_0$ at time t_0, finds the best possible control policy over the time horizon $\tau := [t_0, t_p]$. Such optimization problem can be posed as a general non-linear problem as follows:

$$\underset{x(\cdot), u(\cdot)}{\text{minimize}} \quad \int_{t_0}^{t_p} L(x(t), u(t))dt \qquad (1a)$$

$$\text{subject to} \quad \dot{x}(t) - F(x(t), u(t)) = 0, \quad t \in [t_0, t_p], \quad (1b)$$

$$x(0) - \bar{x}_0 = 0, \qquad (1c)$$

$$h(x(t), u(t)) \geq 0 \quad t \in [t_0, t_p], \quad (1d)$$

where the initial value is enforced by (1c), (1b) guarantees the system dynamics and (1d) represent some general path constraints. A closed loop optimal control problem is obtained by introduction of instantaneous feedback and repeated solution of the open loop OCP Diehl et al. (2002a), Diehl et al. (2002b), Leducq et al. (2006). One could take many different approaches to solving this optimization problem. A linear model predictive control (MPC) approach has been presented among others in Larsen (2005), where the authors focus on set-point optimization. In Shafiei et al. (2013), Hovgaard et al. (2011), Hovgaard et al. (2012), authors present various forms of linear economic MPC for supervisory control. In Pedersen et al. (2014), Pedersen et al. (2013), the authors use a "leaky bucket" model for high level representation of groups of refrigeration units and solve the optimization problem using linear economic MPC as well. Non-linear MPC for vapour compression cycle system has been demonstrated in Leducq et al. (2006). The authors use a multiple shooting method with an explicit Runge Kutta of order 4 integrator for the discretization of system dynamics. Optimization of a commercial refrigeration system with non convex objective function has been presented in Hovgaard et al. (2012). In this paper, we focus on non-linear model based direct methods, direct collocation method is employed Quirynen and Diehl (2015), which is a combination of collocation with multiple shooting.

1.2 Main Contributions

The main contributions of this paper are as follows.

- Modelling and investigation of presented refrigeration system with heat recovery (Chapter II).
- Because of the particular configuration of the system a discontinuity in the input condenser temperature occurs. Smooth model of temperature both for two-phase and saturated gas regions is developped (Chapter III).
- It has been shown that refrigeration system with heat recovery and advanced controller, that enables high pressure control has a negative operational cost. Comparison has been made of the system behaviour under two objective function. First denoted as L_1 and named as *Minimum Consumption* describes the overall operational cost of electrical devices. Second objective function denoted as L_2 and named as *Prosumption* describes the operational cost together with the revenue in connection with reclaimed and sold heat.
- Designing a direct collocation non-linear model predictive controller (NMPC) for refrigeration system with heat recovery (Chapter IV and V).

1.3 Paper Organisation

This paper is organised in the following manner. In *Section II* a non standard configuration of the refrigeration system with heat waste reclaim is presented and differences compared to a typical refrigeration system are explained. First principal models of the system are shown. *Section III* takes up the problem of the discontinuous dynamics of the gas cooler input temperature and presents a way of overcoming such issues. The direct collocation method that has been used is described in *Section IV*. The construction of the objective function, taken optimization procedure and some of the results are given in *Section V*. Acknowledgements and conclusions can be found in *Section VI* and *Section VII*, respectively.
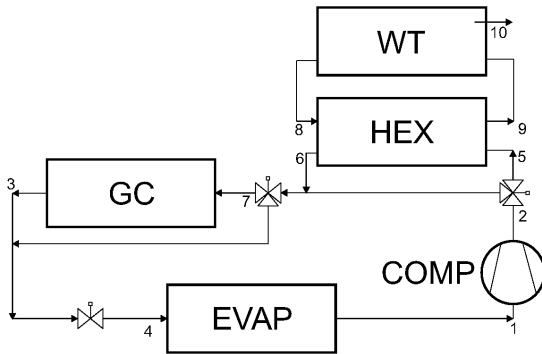
2. REFRIGERATION SYSTEMS DESCRIPTION

Fig. 1. Schematic diagram of refrigeration system with one loop heat waste recovery and thermal storage (WT)

2.1 Assumptions

When modelling the evaporator, we assume that the temperature of the refrigerated goods is the same as the temperature in the display case (Larsen (2005) and Pedersen et al. (2013)); hence, we do not take the heat transfer between evaporator-air and air-food into consideration. Furthermore, we disregard the dynamics of the expansion valve, and model the evaporator assuming that cooling capacity can be controlled as in Shafiei et al. (2013). We assume that the refrigerant mass flow $\dot{m}_r$ can be treated as a control variable. Furthermore, we assume a superheat temperature of $T_{sh} = 10$ and no sub cooling. The indoor temperature T_{ind} that takes part in the description of the cooling demand from the refrigeration system $UA_{mt}(T_{ind} - T_{mt})$ is assumed to be constant and treated as a known disturbance. Moreover, it is assumed that there is no pressure loss in the pipes between the compressor and over the three way valve, $P_{hi} = P_c$. A vapour compression cycle (VCC) system with CO_2 ($R744$) as a refrigerant, which works in the sub critical mode is examined. We constrain the system and do not allow it to work above the critical point. In particular, for CO_2, the critical temperature $T_{crit} = 31.95\,°C$ and pressure $P_{crit} = 73.8\,Bar$. The gas cooler electrical fan, the water pump that produces the mass flow $\dot{m}_c$ in the cooling loop and the compressor are all assumed to be of variable speed types. Furthermore, constant pressure across the water pump is assumed.

2.2 One evaporator, one gas cooler refrigeration system

Four main processes can be distinguished that describe the operation of a typical refrigeration unit. The given process numbers directly corresponds to Fig. 1 and 2.

Evaporation 4-1 The refrigerant that enters the evaporator, evaporates absorbing heat from the surroundings. Assuming that we use a medium temperature display case its air temperature T_{mt} dynamics can be described as in (2). The control over T_{mt} can be facilitated by delivering the specific amount of the cooling capacity $\dot{Q}_e$ (3) which would counteract the heat load $\dot{Q}_{load}$ (4). Knowing that the refrigerated goods need to be kept in between $1 \leq T_{mt} \leq 5\,[°C]$, one has flexibility of changing the delivered $\dot{Q}_e$. The T_{mt} bounds indirectly induce upper and lower limits on $\dot{Q}_e$ and $\dot{m}_r$. Note, that the display case can be viewed as a thermal storage with the capacity described by the mass M_{mt} and the specific heat c_{pmt} Biegel and Stoustrup (2012), Biegel et al. (2014), Pedersen et al. (2014), Rahnama et al. (2013), Shafiei et al. (2013), Vinther et al. (2013).

$$c_{pmt}M_{mt}\dot{T}_{mt} = \dot{Q}_{load} + \dot{Q}_e \qquad (2)$$

$$\dot{Q}_e = \dot{m}_r(h_{ei}(P_e) - h_{eo}(P_c)) \qquad (3)$$

$$\dot{Q}_{load} = UA_{evap}(T_{amb} - T_{mt}) \qquad (4)$$

where, $\dot{m}_r$ is the refrigerant mass flow, h_{eo} and h_{ei} are the evaporator outlet and inlet enthalpies, respectively. T_{amb} is the ambient air temperature.

Compression 1-2 Saturated gas that enters the compressor is pressurized. The work done by the compressor $\dot{W}_{comp}$ is given by (5). Assuming constant ΔT_{sh}, $\dot{W}_{comp}$ value depends on the evaporation and compressor output pressures P_e and P_c as well as the mass flow $\dot{m}_r$.

$$\dot{W}_{comp} = \frac{1}{1 - f_q}\dot{m}_r(h_{gci}(P_c) - h_{eo}(P_e)) \qquad (5)$$

where, h_{gci} is the enthalpy at the inlet to the gas cooler.

Condensation 2-3 High-pressure refrigerant flows through the gas cooler where it is being cooled down. The amount of energy that needs to be rejected $\dot{Q}_c$ is dictated by the following first law of thermodynamics.

$$\dot{Q}_c = \dot{Q}_e + \dot{W}_{comp} - f_q \dot{W}_{comp} \qquad (6)$$

where, $\dot{Q}_e$ is the cooling capacity of the evaporator, $\dot{W}_{comp}$ is the work done by the compressor and f_q is the heat loss coefficient which describes the heat fraction of the compressor work that is being transmitted to the surroundings Sonntag, Richard Edwin and Borgnakke, Claus and Van Wylen, Gordon John and Van Wyk (1998)

Expansion 3-4 The refrigerant is de-pressurized through the expansion valve. So called isenthalpic expansion dictates that enthalpies at points 3 and 4 are equal.

2.3 Refrigeration system with one loop heat waste recovery

The system shown in Fig. 1 contains an additional mean of cooling the refrigerant, than would standard refrigeration system described in 2.2 posses. An additional water cooled heat exchanger (HEX), three way valve for splitting the refrigerant and an additional expansion valve have been used. This results in the following modifications of **Condensation 2-3** .

Water Cooling 2-6 Refrigerant which has been redirected by the three way valve enters heat exchanger (HEX) and is being cooled down. The HEX can be divided into primary side - hot side describing the dynamics of the refrigerant leaving HEX on the refrigeration system side. The ordinary differential equation that describes the dynamics of the enthalpy and the output of the HEX hot side h_{ho} is as follows.

$$M_{ho} \dot{h}_{ho} = d \dot{m}_r (h_{hi}(P_c) - h_{ho}) - \mathrm{UA}_h (T_{hi}(P_c) - T_{wall}), \qquad (7)$$

where, T_{hi} and h_{hi} are the hot side refrigerant temperature and enthalpy, rspectively, at the output of the compressor. Both T_{hi} and h_{hi} are found using regression models of CO_2 refrigerant properties. Furthermore d describes the opening degree of the three way valve, $0 \leq d \leq 1$. Secondary side - cold side of HEX is described by the water temperature that enters the cold side of the HEX T_{ci} (9) and the water temperature at the outlet of HEX T_{ci} (8).

$$c_{pw} M_{co} \dot{T}_{co} = c_{pw} \dot{m}_c (T_{ci} - T_{co}) + \mathrm{UA}_c (T_{wall} - T_{co}) \qquad (8)$$

$$c_{pw} M_{ci} \dot{T}_{ci} = c_{pw} \dot{m}_c (T_{ci} - T_{co}) - \mathrm{UA}_c (T_{co} - T_{wt}) \qquad (9)$$

$$c_{pw} M_{wall} \dot{T}_{wall} = \mathrm{UA}_h (T_{hi} - T_{wall}) - \mathrm{UA}_c (T_{wall} - T_{co}) \qquad (10)$$

Furthermore the HEX wall temperature T_{wall} is described in (10) and the heat transfer coefficients UA_c, UA_h take the following forms

$$UA_c = UA_{c_{nom}} \dot{m}_c / \dot{m}_{c_{nom}} \qquad (11)$$

$$UA_h = UA_{h_{nom}} \dot{m}_h / \dot{m}_{h_{nom}} . \qquad (12)$$

Three way joining and expansion valves 6-7. Because of the mass flow split at point 2, see Fig. 1 and 2, it is necessary to introduce (13) that describes the enthalpy at the gas cooler input h_{gci}, just after the mass flow joining.

$$h_{gci} = d \dot{m}_r h_{ho} + (1 - d) \dot{m}_r h_{hi} . \qquad (13)$$

Gas Cooler 7-3 The refrigerant can be cooled by either gas cooler (GC) or HEX, or the cooling can be shared by both of them. The ODE's that describe the dynamics of the gas cooler output enthalpy h_{gco} (14) and air temperature T_{gca} (15) are as follows.

$$M_{gc} \dot{h}_{gco} = \dot{m}_r (h_{gci} - h_{gco}) - UA_{cond}(T_{gci} - T_{gca}) \qquad (14)$$

$$M_{gca} \dot{T}_{gca} = \dot{m}_{gca} (T_{amb} - T_{gca}) + \frac{UA_{cond} (T_{gca} - T_{gci})}{c_{pair}}, \qquad (15)$$

where $\dot{m}_{gca}$ is a control variable and T_{gci} is an estimated temperature at the input to the gas cooler. A detailed description of the modelling approach taken for the T_{gci} is presented in chapter III.

2.4 Thermal storage

When the refrigerant flows through the HEX the heat waste recovery can be obtained. Water that is pumped through the secondary side of the HEX cools down the refrigerant and transports the reclaimed heat to the water tank (WT). The dynamics of the water storage temperature is described by the following equation:

$$M_{wt} c_{pw} \dot{T}_{wt} = UA_c (T_{co} - T_{wt}) - \dot{m}_d c_{pw} (T_{wt} - T_{ind}) . \qquad (16)$$

The water tank temperature consist of a term that describes the heat transfer from the heat recovery water loop $UA_c (T_{co} - T_{wt})$ and a term $\dot{m}_d c_{pw} (T_{wt} - T_{ind})$, that describes amount of heat discharged from the water tank.
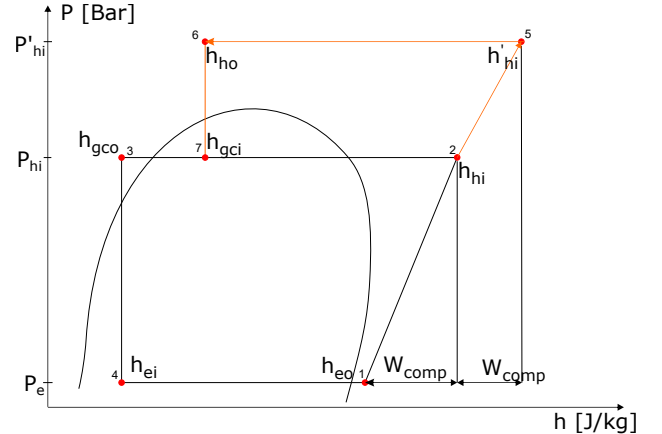

Fig. 2. Vapour Compression Rankine Cycle for refrigeration system with $R744$ (CO_2) refrigerant with heat waste recovery ($d = 1$ case).

3. SUBCRITICAL CO_2 PROPERTIES MODELLING

In this paper the physical model of the systems is utilized in combination with a model predictive method as a means of providing supervisory control. Introduction of the additional water cooled heat exchanger requires that an accurate description of the systems behaviour at point 2, 5, 6 and 7 is provided, see Fig. 2. The focus has been put on creating a model of the temperature just after the isenthalpic expansion, after the mass flow joining T_{gci}, at point 7. T_{gci} exhibits significantly different dynamics depending on the operation point of the system. In the mixed liquid and gas region (L+G) T_{gci} is constant and can be approximated as the linear function of enthalpy

$T_{\mathrm{gci}_{\mathrm{LIN}}} = p_1 h + p_2$. In the saturated gas region the non-linear dynamics of T_{gci} has been successfully approximated using the second order polynomial $T_{\mathrm{gci}_{\mathrm{NL}}} = p_3 h^2 + p_4 h + p_5$. $T_{\mathrm{gci}_{\mathrm{LIN}}}$ and $T_{\mathrm{gci}_{\mathrm{NL}}}$ have one common point that is described by the saturation curve and this point is met only if $P_{\mathrm{gci}} = P_{\mathrm{hi}}$ (when point 2 = 5). Whenever $P_{\mathrm{hi}} > P_{\mathrm{gci}}$, $T_{\mathrm{gci}_{\mathrm{NL}}}$ will enter the mixed liquid and gas region at a higher temperature than the temperature for $T_{\mathrm{gci}_{\mathrm{LIN}}}$. In such cases a discontinuity in temperature occurs.

In order to illustrate it $T_{\mathrm{gci}_{\mathrm{LIN}}}$ for $P_{\mathrm{gci}} = 50 [Bar]$, together with $T_{\mathrm{gci}_{\mathrm{NL}}}$ for pressures in between 50 and $70 [Bar]$ as well as the saturation curve have been plotted in Fig. 3. On the left from the saturation curve (black), the linear dynamics of T_{gci} for mixed liquid and gas region (red) have been plotted. For $P_{\mathrm{gci}} = 50$ $T_{\mathrm{gci}_{\mathrm{LIN}}} = 14.28 [^\circ C]$ and is constant throughout the whole mixed liquid and gas region. On the right side of the saturation curve T_{gci} enters the saturated gas region where it behaves in non-linear fashion. Assuming $P_{\mathrm{hi}} = 70$, the temperature entering the mixed liquid and gas region is $28.7 [^\circ C]$. The higher pressure difference the larger discontinuity jump in temperature can be expected. The saturation curve for pressures in between 50 and $70 [Bar]$ is approximated as a second order polynomial $h_{\mathrm{sat}} = r_1 P_{\mathrm{hi}}^2 + r_2 P_{\mathrm{hi}} + r_3$.
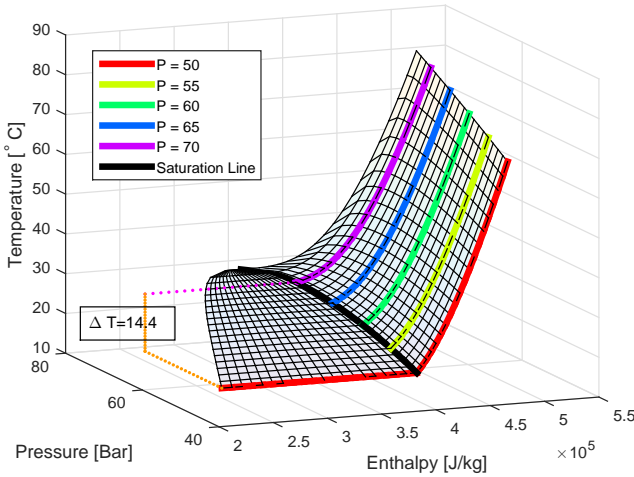

Fig. 3. Two dynamics of refrigerant temperature and occurring discontinuity at the saturation curve.

3.1 Sigmoid Function

Denoting T_{LIN} as a linear function that describe the temperature in the mixed gas region, T_{NL} as the function that describe temperature in the saturated region, one can construct the following continuous function that describe the smooth transition in between T_{LIN} and T_{NL}.

$$T_{\mathrm{TOT}} = (1 - \sigma) T_{\mathrm{LIN}} + \sigma T_{\mathrm{NL}} \qquad (17)$$

$$\sigma = \frac{1}{1 + \exp(-\frac{h - h_{\mathrm{sat}}}{\alpha})} \qquad (18)$$

where, the σ function has the form as in (18) and it smoothly varies in between zero and one. Moreover, h_{sat} is the enthalpy at which the transition occurs and α is a friction fanning factor that represents the smoothness of the transition. A linear models for the mixed gas and liquid region T_{LIN} and a non-linear for saturated gas region

T_{NL} have been acquired. The T_{NL} regression models for different values of pressure P_{hi} have been obtained. In order to acquire a more general surface model for the saturated gas region we approximate p_1, p_2 and p_3 as a function of pressure P_{hi}. Furthermore, the enthalpy h_{sat} at which the discontinuity occurs is modelled. The resulting models are put together in order to create a smooth non-linear model (17) that describes the temperature as a function of enthalpy in both regions of interest.

4. DIRECT OPTIMAL CONTROL METHODS: DIRECT COLLOCATION

In this paper we solve an optimal control problem (OCP) of the form (1a)-(1d) using the direct collocation method. Throughout the simulations, zero order hold discretization of control variables is assumed.

On each discrete time interval $[\tau_{\mathrm{i}}, \tau_{\mathrm{i}+1}]$ the collocation method Quirynen and Diehl (2015) approximates the state trajectories $x(\tau)$ with Lagrange polynomials $P_{\mathrm{i,k}}(\tau)$ of order K. In order to approximate the dynamics $\dot{x} = F(x, u)$ (1b) additional time grid is introduced, such that $\{\tau_{\mathrm{i,0}}, ..., \tau_{\mathrm{i,K}}\} \in [\tau_{\mathrm{i}}, \tau_{\mathrm{i}+1}]$.

$$x(\theta_{\mathrm{i}}, \tau) = \sum_{k=0}^{K} \theta_{\mathrm{i,k}} \cdot P_{\mathrm{i,k}}(\tau) \qquad (19)$$

where, $x(\theta_{\mathrm{i}}, \tau_{\mathrm{i,j}}) = \theta_{\mathrm{i,j}}$, $j = \{1, ..., K\}$ and P is a polynomial basis. Note that $\theta_{\mathrm{i,k}}$ is treated as additional optimization variable and can be adjusted. Furthermore the following collocation constraints needs to be introduced:

$$x(\theta_{\mathrm{i}}, \tau_i) = \theta_{\mathrm{i,0}} = x_{\mathrm{i}} \qquad (20)$$

$$\sum_{k=0}^{K} \theta_{\mathrm{i,k}} \cdot \dot{P}_{\mathrm{i,k}}(\tau) = F(\theta_{\mathrm{i,j}}, u_{\mathrm{i}}) \qquad (21)$$
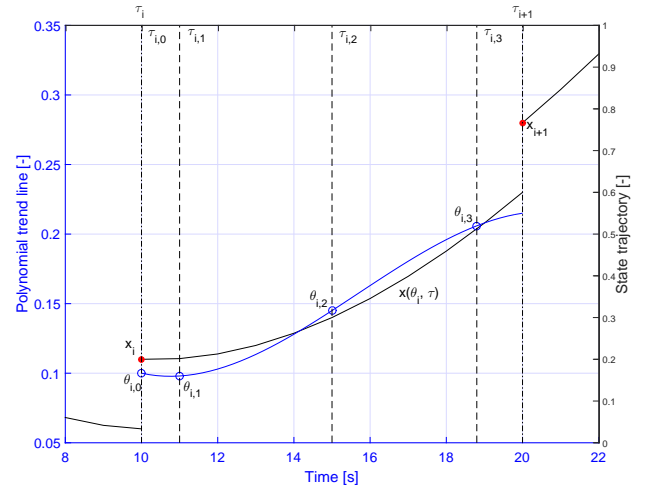

Fig. 4. Collocation General Idea

Fig. 4 illustrates the idea behind the collocation method. The black line represents one interval of the arbitrary state trajectory and the blue line the polynomial that tries to approximate the state trajectory. Additional optimization variables $\theta_{\mathrm{i,k}}$ are introduced and their values are chosen such that corresponding polynomials $P_{\mathrm{i,k}}(t)$ approximates the state trajectory as well as possible. The points $\theta_{\mathrm{i,k}}$

on Fig. 4 will move towards the black line in order to provide best fit. The choice of number of points defines how well the state trajectory can be approximated. It is necessary to enforce the continuity on the shooting intervals. Furthermore in order to achieve a proper fit we need to impose the integration constraints (20) and (21), which forces the derivative of the polynomial to be equal to the value of the approximated state trajectory at the equivalent points.

In this paper collocation based integrator together with multiple shooting is used. Such form is often called as direct collocation in which collocation integrator is put together with its constraints to the NLP solver.

5. SIMULATIONS

All simulations are done using MATLAB Matlab (2015) and the symbolic framework for algorithmic differentiation and numeric optimization CasADi Andersson (2013). The interior point method solver Ipopt Wachter (2006) is used, with the linear solver $MA57$. Direct collocation method is used with three Legendre collocation points. All simulations have been carried out with a total simulation time of $24\,[h]$, a sampling time of $t_s = 5\,[min]$ and a prediction horizon of $t_p = 60\,[min]$. The objective function is constructed such that it consists of three terms

$$\Phi = \Phi_1 - \Phi_2 + \Phi_3 \qquad (22)$$

where,

$$\Phi_1 = \int_{t_0}^{t_p} (p_1(t)(\dot{W}_{comp}(t) + \dot{W}_{gcf}(t) + \dot{W}_{cp}(t) + \dot{W}_{dp}(t))dt \qquad (23)$$

describes the operational cost of the electrical devices,

$$\Phi_2 = \int_{t_0}^{t_p} p_2 \dot{Q}_{sold}(t)\, dt \qquad (24)$$

describes the cost of the sold thermal energy, and

$$\Phi_3 = \int_{t_0}^{t_p} (R_1(X/X_{max})^2 + R_2(U/U_{max})^2)dt, \qquad (25)$$

describes the penalties for our states, controls and restrictions regarding the rate of power change in our system.

In the expressions above, $\dot{W}_{comp} = \beta\dot{m}_r(h_{hi} - h_{eo})$ describes the compressor power consumption. $\dot{W}_{gcf} = (\kappa_1\dot{m}_{gca}^2)$ stands for the gas cooler air fan power consumption, $\dot{W}_{cp} = \kappa_2\dot{m}_c$ and $\dot{W}_{dp} = \kappa_3\dot{m}_d$ for the power consumption of two water pumps used in the heat recovery loop. p_1 and p_2 are the electricity and district heating prices. Furthermore, R_1 and R_2 are diagonal weight matrices, X and U are matrices with elements of state vector x and control vector u on the diagonal, respectively, and X_{max} and U_{max} are diagonal matrices that contain the maximum values of states and control signals, respectively. The non-convex term $\dot{W}_{comp}$ has been replaced by a slack variable.

5.1 Objective Function

Two objective functions L_1 and L_2 were taken under consideration.

$$L_1 = \Phi_1 + \Phi_3 \qquad (26)$$
$$L_2 = \Phi_1 - \Phi_2 + \Phi_3 \qquad (27)$$

Objective function L_1 is named as the *Minimum Consumption* and it describes the overall operational cost of electrical devices. The L_2 is named as the *Prosumption* and describes the revenue in connection with reclaimed and sold heat. The price information of heating p_2 is constant throughout the simulations. In Denmark, the heating prices vary depending on the region. Its value can oscillate in between 42 and $161\,[eur/MWh]$ http://energitilsynet.dk (March 2015). For the purpose of simulations, value of the heating price has been set to $p_2 = 50$;

5.2 Results

The proposed objective functions L_1 and L_2 were compared in the following manner.

- **A.** The total power consumption described by term Φ_1 in (23) is compared, see Fig. 5.
- **B.** The total operational cost for L_1 and L_2 is compared, assuming that in both cases reclaimed heat has been sold, see Fig. 6.

The proposed construction of the L_2 objective function minimizes the terms Φ_1, Φ_3 and maximises term Φ_2. Since p_2 has larger value than the maximum value of p_1, the term Φ_2 dominates the objective function. In other words, L_2 aims at maximizing the amount of reclaimed and sold heat waste. As a result the compressor output pressure and refrigerant mass flow are kept at their maxima, and the display case temperature at its minimum. As for L_1, it exploits the electricity price information and find optimal system trajectories according to electricity price forecasts. On average the total power consumption when using L_1 is lower by 40%. On the other hand, when assuming that the heat is sold when using both L_1 and L_2 objective functions, it turns out that the system has negative operational cost. In the case when L_1 is used daily revenue is about $7.9\,[eur]$, for L_2 it is $11.9\,[eur]$.

6. CONCLUSIONS

When examining a refrigeration systems with just air cooling and without the heat recovery, usually the compressor output pressure P_{hi} is not treated as a control variable, but instead, it is only adjusted according to the changes in the ambient temperature. When heat reclaim is introduced, the control over P_{hi} brings up additional flexibility to the system and increases the refrigeration system's potential for production of heat Q_c. The mechanism of heat recovery has been explained in the paper. Moreover, the continuous temperature model for two-phase and saturated gas regions has been derived. Furthermore direct collocation method has been presented and used. Higher revenue might be achieved for larger systems, with more medium display cases and low temperature freezers. Further increase might be achieved by operating in the supercritical region. More results, all constants, parameters
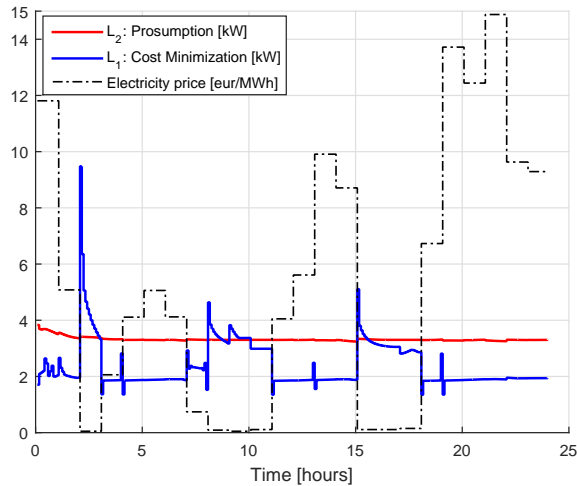
Fig. 5. Comparison of system operational cost for L_1: *Cost Minimization* and L_2: *Prosumption* objective functions.
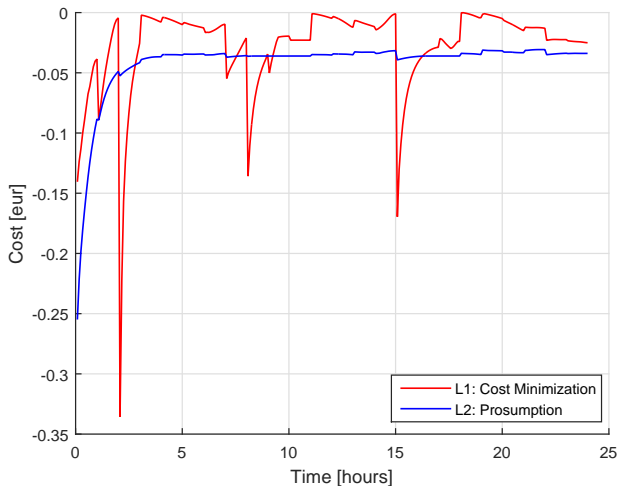

Fig. 6. Total operational cost comparison for L_1 and L_2 objective functions.

values together with simulation files can be found at: $http : //kom.aau.dk/project/edge/repository/IFAC\_2017/$.

7. ACKNOWLEDGMENTS

REFERENCES

Andersson, J. (2013). *A General Purpose Software Framework for Dynamic Optimization*. Ph.D. thesis, Arenberg Doctoral School, KU Leuven.

Biegel, B. and Stoustrup, J. (2012). Model predictive control for power flows in networks with limited capacity. *American Control . . .* , 2959–2964.

Biegel, B., Westenholz, M., Hansen, L.H., Stoustrup, J., Andersen, P., and Harbo, S. (2014). Integration of flexible consumers in the ancillary service markets. *Energy*, 67, 479–489. doi:10.1016/j.energy.2014.01.073.

Diehl, M., Bock, H., Schlöder, J.P., Findeisen, R., Nagy, Z., and Allgöwer, F. (2002a). Real-time optimization and nonlinear model predictive control of processes governed by differential-algebraic equations. *Journal of Process Control*, 12, 577–585. doi:10.1016/S0959-1524(01)00023-3.

Diehl, M., Findeisen, R., Schwarzkopf, S., Uslu, I., Allgöwer, F., Bock, H.G., Gilles, E.D., and Schlöder, J.P. (2002b). An Efficient Algorithm for Nonlinear Model Predictive Control of Large-Scale Systems Part I: Description of the Method. *at - Automatisierungstechnik*, 50(12_2002), 557. doi:10.1524/auto.2002.50.12.557.

Hovgaard, T.G., Larsen, L.F.S., Edlund, K., and Jørgensen, J.B. (2012). Model predictive control technologies for efficient and flexible power consumption in refrigeration systems. *Energy*, 44(1), 105–116. doi:10.1016/j.energy.2011.12.007.

Hovgaard, T.G., Larsen, L.F.S., and Jorgensen, J.B. (2011). Flexible and cost efficient power consumption using economic MPC a supermarket refrigeration benchmark. In *Proceedings of the IEEE Conference on Decision and Control*, 848–854. doi:10.1109/CDC.2011.6161162.

http://energitilsynet.dk (March 2015). Energitilsynet prisstatistik for fjernvarmeomradet.

Larsen, L.F.S. (2005). *Model Based Control of Refrigeration Systems Lars Finn Sloth Larsen*.

Leducq, D., Guilpart, J., and Trystram, G. (2006). Nonlinear predictive control of a vapour compression cycle. *International Journal of Refrigeration*, 29(5), 761–772. doi:10.1016/j.ijrefrig.2005.12.005.

Matlab (2015). *version R2015a*. The MathWorks Inc.

Pedersen, R., Schwensen, J., Biegel, B., Stoustrup, J., and Green, T. (2014). *Aggregation and control of supermarket refrigeration systems in a smart grid*, volume 19. IFAC. doi:10.3182/20140824-6-ZA-1003.00268.

Pedersen, R., Schwensen, J., Sivabalan, S., Corazzol, C., Shafiei, S.E., Vinther, K., and Stoustrup, J. (2013). Direct Control Implementation of a Refrigeration System in Smart Grid.

Quirynen, R. and Diehl, M. (2015). Lifted implicit integrators for direct optimal control. *Conference on Decision and Control (CDC)*, (Cdc), 3212–3217.

Rahnama, S., Stoustrup, J., and Rasmussen, H. (2013). Integration of heterogeneous industrial consumers to provide regulating power to the smart grid. In *Proceedings of the IEEE Conference on Decision and Control*, 6268–6273. doi:10.1109/CDC.2013.6760880.

Shafiei, S.E., Stoustrup, J., and Rasmussen, H. (2013). A supervisory control approach in economic MPC design for refrigeration systems. 1565–1570.

Sonntag, Richard Edwin and Borgnakke, Claus and Van Wylen, Gordon John and Van Wyk, S. (1998). Fundamentals of thermodynamics. 6.

Vinther, K., Chandan, V., and Alleyne, A.G. (2013). Learning / Repetitive Control for Building Systems with Nearly Periodic Disturbances. (ii).

Wachter, A.L.T.B. (2006). On the Implementation of a Primal-Dual Interior Point Filter Line Search Algorithm for Large-Scale Nonlinear Programming. *Mathematical Programming*, 106(1), 25—-57.